Lasers in Surgery and Medicine 26:145–157 (2000)

Bioheat Transfer Analysis of Cryogen Spray Cooling During Laser Treatment of Port Wine Stains

T. Joshua Pfefer, PhD,[1]* Derek J. Smithies, PhD,[2] Thomas E. Milner, PhD,[1,2] Martin J.C. van Gemert, PhD,[3] J. Stuart Nelson, MD, PhD,[2] and Ashley J. Welch, PhD[1]

[1]Biomedical Engineering Program, The University of Texas at Austin, Austin, Texas, 78712
[2]Beckman Laser Institute and Medical Clinic, University of California, Irvine, California, 92715
[3]Laser Center, Academic Medical Center, Amsterdam, 1105 AZ, The Netherlands

Background and Objective: **The thermal response of port wine stain (PWS) skin to a combined treatment of pulsed laser irradiation and cryogen spray cooling (CSC) was analyzed through a series of simulations performed with a novel optical-thermal model that incorporates realistic tissue morphology.**
Study Design/Materials and Methods: **The model consisted of (1) a three-dimensional reconstruction of a PWS biopsy, (2) a Monte Carlo optical model, (3) a finite difference heat transfer model, and (4) an Arrhenius thermal damage calculation. Simulations were performed for laser pulses of 0.5, 2, and 10 ms and a wavelength of 585 nm. Simulated cryogen precooling spurts had durations of 0, 20, or 60 ms and terminated at laser onset. Continuous spray cooling, which commenced 60 ms before laser onset and continued through the heating and relaxation phases, was also investigated.**
Results: **The predicted response to CSC included maximal pre-irradiation temperature reductions of 27°C at the superficial surface and 12°C at the dermoepidermal junction. For shorter laser pulses (0.5, 2 ms), precooling significantly reduced temperatures in superficial regions, yet did not effect superficial vessel coagulation. Continuous cooling was required to reduce significantly thermal effects for the 10-ms laser pulse.**
Conclusions: **For the PWS morphology and treatment parameters studied, optimal damage distributions were obtained for a 2-ms laser pulse with a 60-ms precooling spurt. Epidermal and vascular morphology as well as laser pulse duration should be taken into account when planning CSC/laser treatment of PWS. Our novel, realistic-morphology modeling technique has significant potential as a tool for optimizing PWS treatment parameters. Lasers Surg. Med. 26:145–157, 2000.**

Key words: bioheat transfer; cryogen spray cooling; laser-tissue interaction; light propagation; Monte Carlo; numerical modeling; port wine stains; thermal damage

INTRODUCTION

Ideal treatment of port wine stains (PWS) and other cutaneous vascular lesions requires selective thermal necrosis of blood vessels with minimal damage to the normal overlying epidermis and adjacent dermis [1]. Past research into laser treatment of PWS has often involved investigations of alternate laser parameters to reduce collateral damage [2]. Continuous wave lasers

Contract grant sponsor: Office of Naval Research Free Electron Laser Biomedical Science Program; Contract grant number: N00014-91-J-1564; Contract grant sponsor: Albert W. and Clemmie A. Caster Foundation; Contract grant sponsor: Whitaker Foundation; Contract grant number: WF-21025; Contract grant sponsor: National Institutes of Health; Contract grant number: AR43419.

*Correspondence to: T. Joshua Pfefer, PhD, Wellman Laboratories of Photomedicine, Massachusetts General Hospital, Bartlett 722, 55 Fruit Street, Boston, MA 02114.
E-mail: jpfefer@helix.mgh.harvard.edu

Accepted 14 October 1999

such as the argon, which produced extensive regions of dermal and epidermal coagulation, have been replaced by pulsed lasers to limit thermal diffusion during irradiation [3].

Surface cooling has proven effective for reducing collateral thermal injury during vessel photocoagulation in skin [4–6]. Because the epidermis contains the chromophore melanin, light absorption can result in the generation of high temperatures that lead to necrosis and undesired dyspigmentation or scarring. By minimizing superficial temperatures and the duration of high-temperature exposure, thermal injury in the epidermis can be reduced or prevented. Epidermal cooling enables the use of higher radiant exposures and, thus, deeper coagulation of cutaneous vessels. Cooling may also reduce the temperature in superficial blood vessels, decreasing the risk of ablation-induced vessel rupture.

Various skin cooling techniques such as ice [4,5,7], a water-chilled, transparent plate [8], direct water irrigation [5], and water spray [9] have been investigated for use in treatment of vascular lesions. These methods tend to require long exposure durations due to the low surface heat transfer; however, they are suitable for achieving temperature reduction deep within the tissue. A technique that has been shown to be more appropriate for spatially selective cooling of superficial skin regions is cryogen spray cooling (CSC).

In the 1950s, pressurized sprays of cryogen (low boiling point refrigerants such as freon) were implemented to prepare the skin for dermabrasion procedures [10]. In 1983, Welch et al. [5] investigated the use of a freon gas spray to reduce thermal damage during irradiation of porcine skin in vivo with continuous wave argon and Nd:YAG laser irradiation. Although this first application of spray cooling to photocoagulation of cutaneous vessels was not optimized, results indicated that it could provide significant reduction of epidermal and dermal coagulation in comparison to noncooled treatment or direct precooling with ice.

Treatments involving CSC have combined spurts of liquid, nonchlorofluorocarbon refrigerants (from tens to hundreds of milliseconds in duration) with laser irradiation (λ = 585 nm, τ_p ~ 0.5 ms) [6,11]. These studies have involved the release of a refrigerant such as tetrafluoroethane ($C_2H_2F_4$; boiling point = –26.2°C) from a pressurized (~5 atm) canister [11]. A mixture of cryogen and ice accumulate in a thin layer (10–20 μm) on the skin surface. CSC begins to reduce skin temperature within a millisecond of spray onset and the ice/cryogen layer may remain on the skin for hundreds of milliseconds after a 100 ms spurt [12]. Heat transferred from the skin causes the cryogen to evaporate, creating a strong convective effect [13]. Highly transient cooling of the superficial skin regions can lead to surface temperature reductions of 30–40°C for cryogen spurt durations (D_{csc}) of 5–100 ms [14,15]. These studies have indicated that CSC allows the use of increased radiant exposures without epidermal injury, thus allowing deeper coagulation of blood vessels and expediting PWS clearance.

THEORETICAL MODELS OF CRYOGEN SPRAY COOLING

The thermal mechanisms involved in this highly transient process remain only partially understood. Two types of models have been used to investigate CSC: those that simulated cooling alone [14,16] and those that simulated cooling in conjunction with laser heating [15,17]. These models have been one-dimensional (1-D) and simulated tissue morphology by using homogeneous layers. The usefulness of layered geometry models may be limited when attempting to simulate thermal transients in PWS skin, because PWS morphology is highly nonhomogeneous in three dimensions. Specifically, these models were not able to account for the unique optical and thermal effects in and around discrete blood vessels or predict the spatial distribution of thermal damage. Previous models have also assumed homogeneous thermal and damage properties throughout the skin, accounted for the effects of light scattering by using simple approximations, and neglected the effect of heat transfer during the laser pulse [14,15,17]. Previous simulations of CSC/laser treatment have only been performed for τ_p ~ 0.5 ms, whereas clinical treatment increasingly uses lasers with pulse durations of 1–10 ms. One previous study investigated the use of liquid nitrogen and water cooling during laser treatment of PWS by using a 2-D, layered-geometry, optical-thermal numerical model [18].

According to Anvari et al., ". . . the optimum cooling strategy needs to be determined on [an] individual patient basis as density of melanosomes as well as depth of the PWS blood vessels vary considerably" [15]. Therefore, modeling-based, patient-specific treatment planning may be useful in optimizing cooling parameters. Additionally, the use of true PWS morphology in simu-

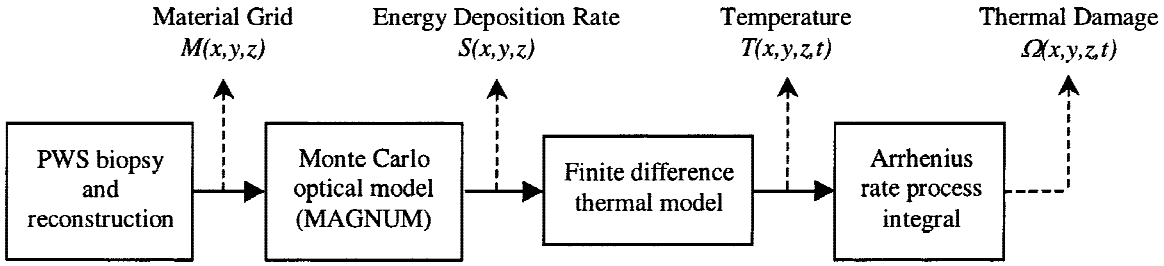

Fig. 1. Flow chart of the modeling process. PWS, port wine stain.

lating the effects of CSC provides a unique perspective on basic optical and thermal laser-tissue interactions during PWS treatment.

CSC is a novel and effective adjunct to PWS treatment. However, to achieve optimal application of CSC, it is important to know how thermal transients and the extent of protection against thermal injury vary with cryogen spurt duration and laser parameters. The purpose of this study is to investigate these basic mechanisms and to assess mathematically the effect of specific CSC spurt durations on irreversible damage in PWS skin components. This has been accomplished by simulating PWS laser treatment (λ = 585 nm; τ_p = 0.5, 2, 10 ms) in conjunction with CSC (precooling) spurts (D_{csc} = 20, 60 ms) and continuous spray cooling.

MATERIALS AND METHODS

The modeling approach used in this study is nearly identical to that described and reported in a previous study of laser treatment of PWS without cooling [19]. As depicted in Figure 1, the model includes a tissue grid that has been generated from a PWS biopsy, which provides information about local tissue type (epidermis, dermis, or blood) and, thus, material property data for the light propagation, heat transfer, and thermal damage modeling components.

The high-resolution computer-based PWS biopsy reconstruction was described previously by Smithies et al. [20]. A portion of the reconstructed volume measuring 268 μm × 312 μm × 460 μm (x,y,z, where z is depth) was used in the present study. This material grid included 52 x–z sections of 134 × 230 voxels each, resulting in a total of approximately 1.6 million rectangular voxels (2 μm × 6 μm × 2 μm). The material grid was identical in size and dimension to the grids used for energy absorption, temperature, and damage distributions.

The 3-D, arbitrary morphology Monte Carlo model used to simulate light propagation in this study has been described and verified previously [21] and implemented by using the aforementioned PWS biopsy reconstruction [19,22]. The primary optical properties — absorption coefficient (μ_a), scattering coefficient (μ_s), scattering anisotropy (g) and index of refraction (n) — used in the present simulations are displayed in Table 1. A single optical simulation is required to calculate the energy deposition rate distribution for a nominal irradiance of 1 W/cm^2. This distribution is then scaled linearly with irradiance to produce the source term (S) for each thermal simulation.

The explicit finite difference technique is used to solve the 3-D transient form of the Fourier heat conduction equation [13]:

$$\rho c \frac{\partial T}{\partial t} = \frac{\partial}{\partial x}\left(k\frac{\partial T}{\partial x}\right) + \frac{\partial}{\partial y}\left(k\frac{\partial T}{\partial y}\right) + \frac{\partial}{\partial z}\left(k\frac{\partial T}{\partial z}\right) + S \qquad (1)$$

where T is temperature (°C), t is time (seconds), S is the heat source term (W/m^3), ρ is density (kg/m^3), c is specific heat (J/kg/°C), and k is thermal conductivity (W/m/°C). The bioheat equation is not used because of the very short time scales and, thus, negligible perfusion effects involved. Adiabatic boundary conditions are applied to the five internal tissue boundaries, whereas a standard Robin convection condition is used to describe heat flow between the superficial tissue layer and the environment. A uniform initial skin temperature of 30°C was assumed. The thermal properties of skin used in these simulations are listed in Table 2 [23].

The primary advantage of the simulations performed for this study lies in the combination of realistic tissue morphology with a surface boundary condition that simulates CSC. In general, processes involving convection with phase change such as the boiling of a cryogen can be approximated by using a convection coefficient (h) of 2.5

TABLE 1. Optical Properties of Skin Components at λ = 585 nm*

	μ_a (cm^{-1})	μ_s (cm^{-1})	g	n
Epidermis	18	470	0.79	1.37
Dermis	2.4	129	0.79	1.37
Blood	191	467	0.99	1.33

*From van Gemert et al. [3].

TABLE 2. Thermal Properties of Skin Components*

	k (W/m/°C)	ρ (kg/m^3)	c (J/kg/°C)
Epidermis	0.21	1200	3600
Dermis	0.53	1200	3800
Blood	0.55	1100	3600

*From Duck [23].

to 100 kW/m^2/°C [13]. For the present study, the convection coefficient (4 kW/m^2/°C) and ambient temperature (–7°C) values from a previous investigation of CSC are implemented [16].

The temporal progression of CSC/laser treatment of PWS was simulated in three phases: (1) a *precooling* phase, involving cryogen cooling (and no laser irradiation) for a duration (D_{csc}) of 0, 20 or 60 ms; (2) a *heating* phase, involving an adiabatic surface and laser irradiation for a duration of (τ_p) 0.5, 2 or 10 ms; and (3) a *relaxation* phase, involving an adiabatic surface and no laser irradiation until temperatures relaxed to below 60°C (at which point the simulation is ended because the damage accumulation rate is minimal). The assumption that cooling terminates at the end of the CSC pulse is a first approximation. A residual ice/cryogen layer may provide post-spray cooling [9,12] although the significance of this effect is likely dependent on spray duration, volume of cryogen released, and other variables. The "continuous cooling" simulation incorporated a second temporal structure in which the convective boundary was implemented starting 60 ms before laser onset and continuing through a 10-ms heating phase and subsequent relaxation to below 60°C.

The Arrhenius rate process equation is used to calculate thermal damage:

$$\Omega(t) = A\int_0^t \exp\left[-\frac{E_a}{RT(\tau)}\right]d\tau \qquad (2)$$

where A is the frequency factor or molecular collision rate (1/s), E_a is activation energy (J/mole), and R is the universal gas constant (8.314 J/mole/K) [24,25]. The thermal damage calculation is implemented as a subroutine in the thermal diffusion model. Two sets of damage coefficients (A, E_a) are used: one for blood (hemoglobin [26]) and another for epidermis and dermis (bulk skin [27]). These values are displayed in Table 3 and Figure 2 for comparison with other relevant data from the literature.

The thermal response of tissue to irradiation at a specific radiant exposure or irradiance level is highly dependent on laser pulse duration. This is seen in the use of higher radiant exposure levels for longer laser pulse PWS treatments. To present more comparable situations, we have altered the radiant exposure based on the tissue thermal response, by using a temperature-based end point in a manner similar to previous theoretical studies [3,28,29]. For each of the three non-CSC cases (D_{csc} = 0 ms and τ_p = 0.5, 2, 10 ms), a radiant exposure was found that produced a maximum end of laser pulse temperature of 150°C (Table 4). This radiant exposure was then used for the corresponding cooling simulations (D_{csc} = 20, 60 ms) for that laser pulse duration. This temperature was chosen because it ensured that significant damage would be produced in the region of the blood vessels without exceeding ablation-level temperatures reported for laser-irradiated tissue [30,31].

RESULTS

The predicted end of laser pulse temperatures and final (post-relaxation phase) coagulation distributions are presented in Figures 3 and 4, respectively. Although results were computed for the entire 3-D tissue volume, data are presented here for a single 2-D section. In Figures 3 and 4, data are presented for pulse durations of 0.5, 2, and 10 ms for the uncooled (D_{csc} = 0) and precooled (D_{csc} = 20, 60 ms) cases.

The temperature distributions immediately after irradiation (Figure 3) show a decreasing level of thermal confinement with increasing laser pulse duration. For τ_p = 0.5 ms, large temperature gradients were predicted at the edge of the epidermis and blood vessels, whereas for longer pulse durations, these gradients decreased and perivascular heating increased. As τ_p lengthened, heat transfer from blood regions necessitated the use of higher radiant exposures to reach an end-point temperature of 150°C. As a result, epidermal temperatures increased with laser

TABLE 3. Rate Process Coefficients*

	A (1/s)	E_a (J/mole)	T_{th} (°C)	Reference
1. Hemoglobin	7.6×10^{66}	455,000	93	[26]
2. Bovine serum albumin	3.2×10^{56}	379,000	90	[37]
3. Aorta	5.6×10^{63}	430,000	91	[38]
4. Bulk skin	7.6×10^{76}	550,000	74	[27]
5. Bulk skin	3.1×10^{98}	628,000	67	[39]

*In the present study, hemoglobin [26] data were used for blood regions and bulk skin [27] for dermis and epidermis. Threshold temperature for coagulation (T_{th}) is listed for a constant temperature exposure duration of 10 ms.

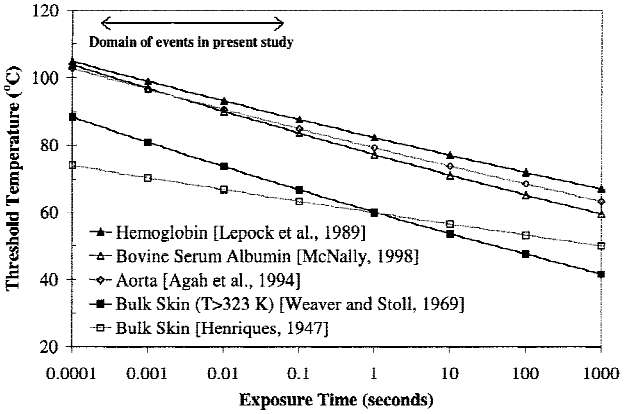

Fig. 2. Graph of time-temperature relationship defined by Arrhenius equation and rate coefficients assuming step temperature changes and well-defined exposure durations.

TABLE 4. Laser Parameters to Produce a Maximum Temperature of 150°C Without Cooling

Pulse duration (ms)	0.5	2.0	10.0
Irradiance (W/cm^2)	6900	3025	1300
Radiant exposure (J/cm^2)	3.45	6.05	13.00

pulse duration until they approached maximum vessel temperatures.

The effect of τ_p on the final (post-relaxation phase) distribution of thermal injury is shown in Figure 4. The duration of the relaxation phase (from the end of irradiation until the maximum temperature fell to below 60°C and the simulation was terminated) increased with laser pulse duration from less than 1 ms for $\tau_p = 0.5$ ms to hundreds of milliseconds for $\tau_p = 10$ ms. Damage distributions show some correlation with the post-irradiation temperatures shown in Figure 3. Coagulation was primarily limited to the blood vessels for $\tau_p = 0.5$ ms, whereas longer pulse durations produced wider regions of perivascular coagulation. Similarly, an increase in pulse duration produced an increase in extent of epidermal coagulation. For $\tau_p = 10$ ms, heat generated in the epidermis and blood diffused into the dermis during and after the laser pulse, causing regions of epidermal and perivascular coagulation to develop into widespread necrosis.

The most obvious result of increased cryogen spurt duration was the elimination of epidermal coagulation for $\tau_p = 2$ ms, from the noncooled case to the $D_{csc} = 20$ ms case. The thickness of perivascular damage in superficial regions was reduced by only a few microns from the uncooled to $D_{csc} = 60$ ms case. Cooling reduced temperatures and thermal injury only in superficial regions for $\tau_p = 0.5$ or 2 ms, whereas for $\tau_p = 10$ ms, it reduced the extent of deeper dermal coagulation. It is likely that much of the dermal injury in the noncooled case was caused by heat that was generated in the epidermis and superficial vessels and diffused into deeper regions after the end of the laser pulse.

The predicted effect of CSC on end of precooling phase temperatures is presented in Figure 5 for durations of 20 ms (black lines) and 60 ms (gray lines). To investigate the effect of spatial variations in thermal properties, two sets of simulations were performed: one in which heterogenous tissue properties were used (thick lines), and one in which the thermal properties of dermis were implemented for all three tissue types (thin lines). In the heterogenous case, 20 ms of cooling caused epidermal temperatures to be reduced by 7–23°C, whereas a 60-ms CSC spurt caused reductions of 12–27°C. The effect of the 60 ms CSC spurt on temperatures below the dermoepidermal junction was more than double that produced by the 20-ms spurt. The magnitude of temperature reduction and gradients in the epidermis were significantly reduced for the homogenous thermal properties case due to the higher values of thermal conductivity and diffusivity in the epidermis. The increased rate of heat conduction led to higher surface temperatures but lower temperatures at and below the dermoepidermal junction for the heterogeneous case. The magnitude of these effects increased with cooling duration.

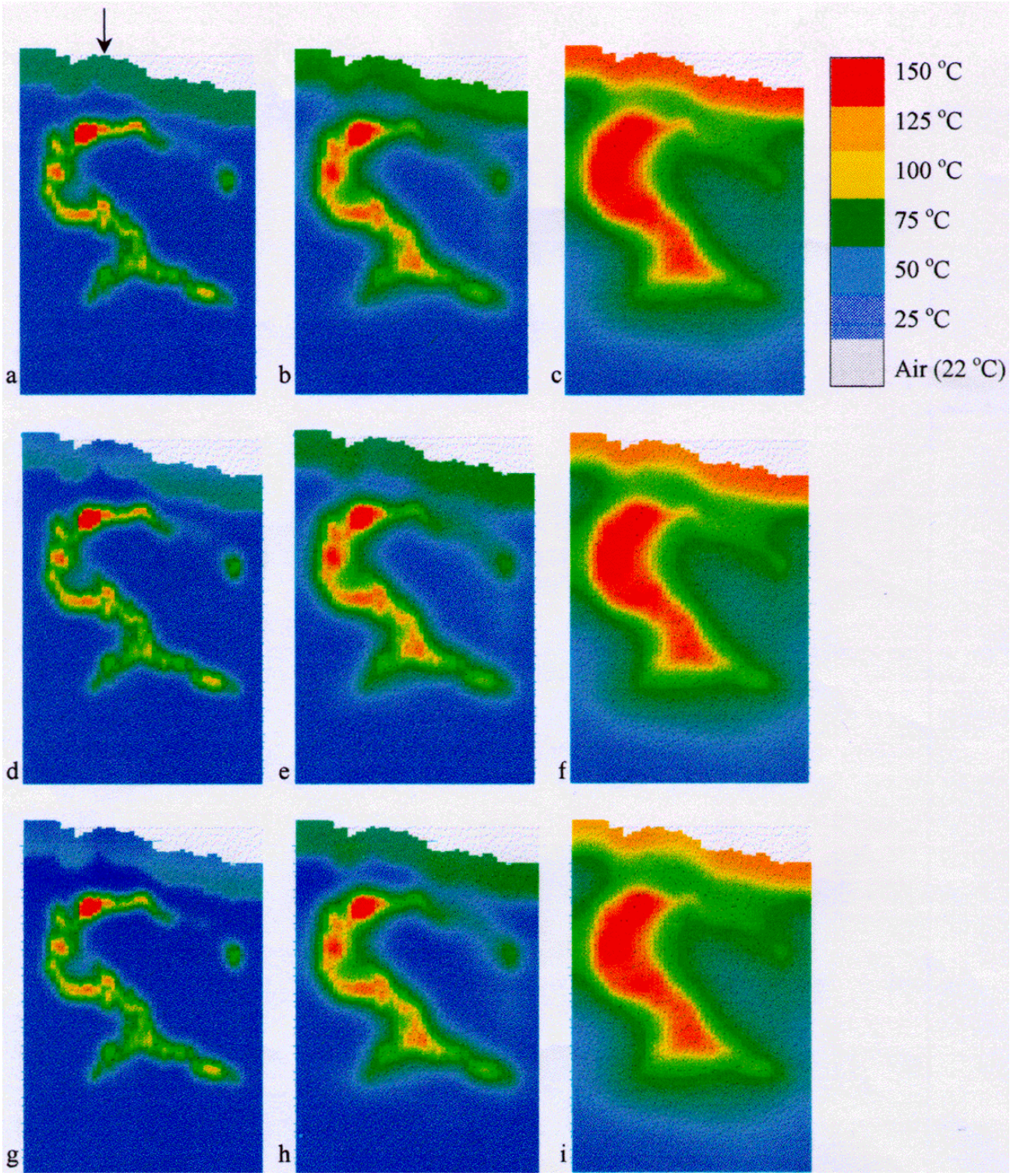

Fig. 3. Temperature distributions immediately after the end of the laser pulse (arrow indicates location of data used in Figs. 5–9). Region shown is 312 μm × 460 μm (width × depth). Radiant exposures are listed in Table 4. (**a**) τ_p = 0.5 ms, no cooling; (**b**) τ_p = 2 ms, no cooling; (**c**) τ_p = 10 ms, no cooling; (**d**) τ_p = 0.5 ms, D_{csc} = 20 ms; (**e**) τ_p = 2 ms; D_{csc} = 20 ms; (**f**) τ_p = 10 ms D_{csc} = 20 ms; (**g**) τ_p = 0.5 ms, D_{csc} = 60 ms; (**h**) τ_p = 2 ms, D_{csc} = 60 ms; (**i**) τ_p = 10 ms, D_{csc} = 60 ms. Arrow in a indicates location of data in Figures 6–8.

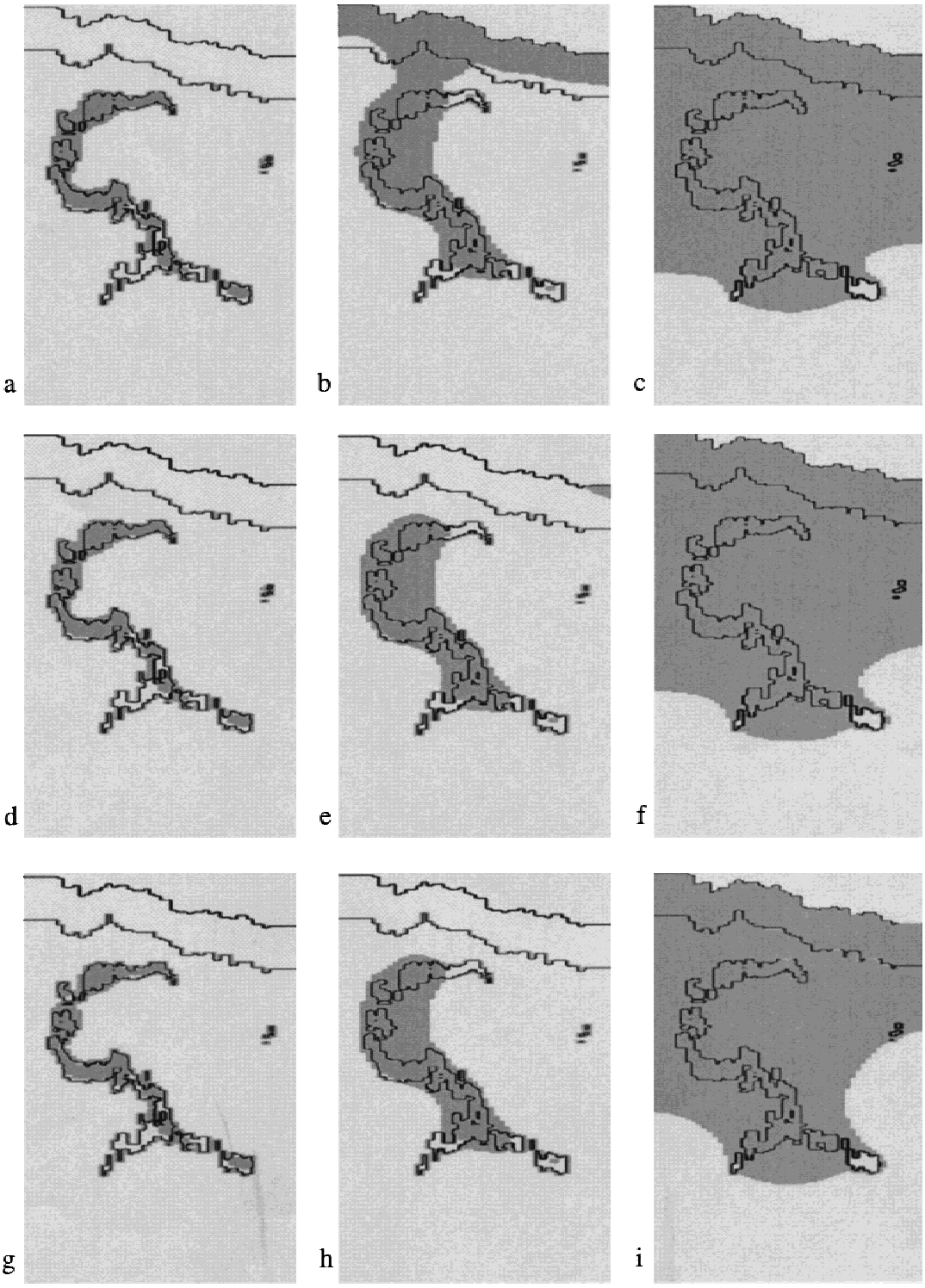

Fig. 4. Distribution of native (light gray) and coagulated (dark gray) tissue after the end of the relaxation phase. Region shown is 312 μm × 460 μm (width × depth). Radiant exposures are listed in Table 4. (**a**) τ_p = 0.5 ms, no cooling; (**b**) τ_p = 2 ms, no cooling; (**c**) τ_p = 10 ms, no cooling; (**d**) τ_p = 0.5 ms, D_{csc} = 20 ms; (**e**) τ_p = 2 ms; D_{csc} = 20 ms; (**f**) τ_p = 10 ms D_{csc} = 20 ms; (**g**) τ_p = 0.5 ms, D_{csc} = 60 ms; (**h**) τ_p = 2 ms, D_{csc} = 60 ms; (**i**) τ_p = 10 ms, D_{csc} = 60 ms.

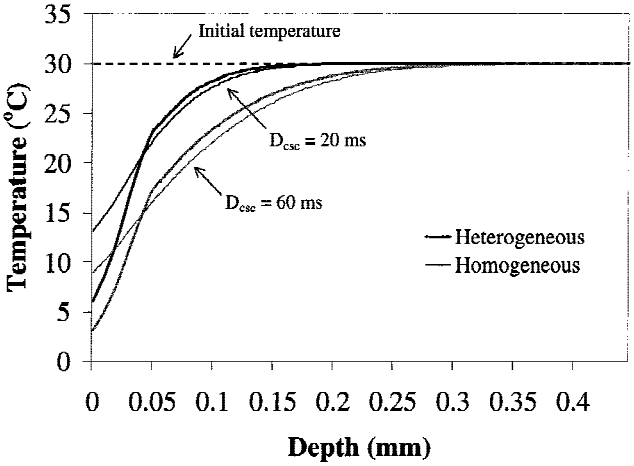

Fig. 5. Comparison of temperature distributions immediately after precooling phase for heterogeneous (thick lines) and homogeneous (thin lines) thermal properties. Cryogen spurts of 20 ms (black lines) and 60 ms (lines) were simulated. Dermoepidermal junction is at a depth of 0.05 mm.

A more quantitative documentation of the end of heating phase temperature distributions for a specific data set (indicated by the arrow in Figure 3a) is presented in Figures 6–8. The most significant CSC-induced temperature reductions (compared with noncooled simulations) occurred within 0.1 mm of the surface. The data in Figure 7 indicate that the CSC-induced epidermal sparing seen for the τ_p = 2-ms case (Fig. 4) was due to decrease in epidermal temperatures from 80 to 60°C. The only cases for which temperature increased significantly with depth across the epidermis were τ_p = 0.5 ms and cooling durations of 20 and 60 ms. This gradient was a remnant from the end of the precooling phase (Fig. 5) but had been reduced in magnitude by heat conduction during the laser pulse. Although temperature reduction at the surface varied significantly with pulse duration (25°C reduction for τ_p = 0.5 ms; 15°C for τ_p = 10 ms), at a depth of 0.05 mm this discrepancy was greatly reduced (12 and 13°C).

The results of a simulation involving continuous cooling are presented in Figures 8 and 9. In this case, CSC began 60 ms before the onset of a 10-ms laser pulse and continued until the very end of the simulation (the end of the relaxation phase). This provided a temperature gradient at the superficial surface before, during, and after the laser pulse, resulting in a significant reduction in superficial temperatures and thermal injury compared with the D_{csc} = 60-ms case. Although continuous cooling resulted in a further reduction in temperature of nearly 60°C near the skin surface, the difference near the dermoepidermal junction was only about 5°C. As a result, only epidermal regions were spared (including regions corresponding to Fig. 8 data). Note that the region spared contains ridges, thus a higher local surface area and an increased rate of cooling.

Because thermal damage is a rate process, and, thus, a function of time and temperature, transient thermal behavior is a critical issue. Surface temperature dynamics are presented in Figure 10 for two cases: τ_p = 2 ms with no cooling and τ_p = 2 ms with D_{csc} = 60 ms. This figure indicates that with or without CSC, temperatures are predicted to decrease at a moderate rate over the first hundred milliseconds after the laser pulse. The initial, relatively constant temperature level in the CSC case was likely due to some diffusion of heat from deeper regions of the epidermis toward the surface.

DISCUSSION

Optical-Thermal Mechanisms

One of the benefits of an arbitrary-morphology model is the ability to account for realistic heterogeneity in thermal properties. Due to the low water content of the epidermis, its thermal conductivity (and possibly diffusivity) is lower than that of dermis [23]. As a result, the effect of the surface boundary is more confined than if homogeneous tissue properties were assumed. This effect is apparent in Figure 5, where the heterogeneous tissue case resulted in lower surface temperatures than the homogeneous (dermis thermal properties) case and higher temperatures at locations deeper than the dermoepidermal junction. Low thermal conductivity also causes heat generated in the epidermis during irradiation to remain in that region, an effect that was exacerbated by the lack of heat loss at the surface after the precooling phase, often resulting in extensive damage in or near the epidermis.

Although the crossover points that occur near the dermoepidermal junction in Figure 5 seem to be a result of an energy balance, this is not strictly true. In fact, the lower surface temperatures in the heterogeneous case produced a weaker temperature differential and reduced convective losses at the surface as well as the total quantity of energy removed. Because the most superficial regions of the epidermis have the least water content, removal of the stratum corneum may decrease the resistance to heat flow and im-

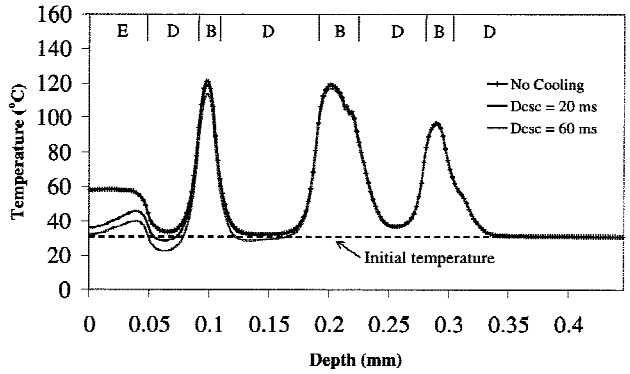

Fig. 6. Temperature distributions immediately after the end of the laser pulse for τ_p = 0.5 ms (H_o = 3.45 J/cm^2) and D_{csc} = 0, 20 and 60 ms. The letters E, D, and B indicate the location of epidermis, dermis and blood regions, respectively.

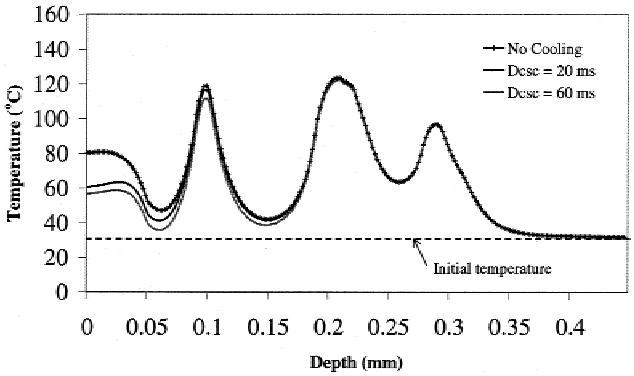

Fig. 7. Temperature distributions immediately after the end of the laser pulse for τ_p = 2 ms (H_o = 6.05 J/cm^2) and D_{csc} = 0, 20, and 60 ms.

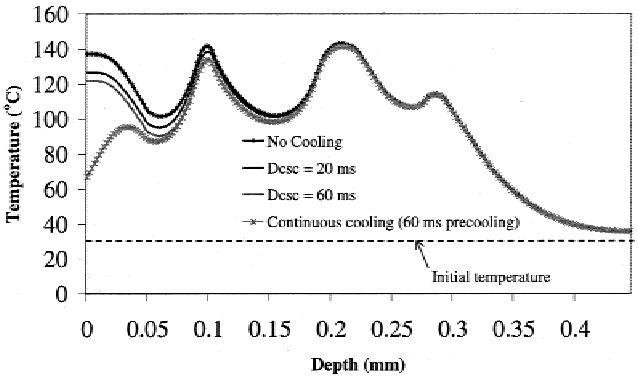

Fig. 8. Temperature distributions immediately after the end of the laser pulse for τ_p = 10 ms (H_o = 13.00 J/cm^2) and D_{csc} = 0, 20, 60 ms, and continuous cooling simulation (CSC began 60 ms before 10 ms laser pulse and continued through heating and relaxation phases).

prove the ability of cryogen to remove heat from epidermal and superficial dermal regions.

Although CSC reduces temperatures throughout the epidermis, end of precooling phase temperature distributions are highly nonuniform across this layer (Fig. 5). For short laser pulses, the post-irradiation temperature distribution across the epidermis maintains this variation (Fig. 6). Because the basal layer is the deepest epidermal layer (epidermal rete pegs may extend into the dermis to a depth of 100 μm) and has the highest melanin content, the subsurface temperatures during CSC/laser treatment may be even greater than predicted. A more realistic, multilayer representation of epidermal morphology, to account for variations in both optical and thermal properties, may yield more accurate predictions [17,32].

Transient surface temperatures (Fig. 10) indicated a greater thermal relaxation rate for the uncooled case (21°C over 100 ms) than for D_{csc} = 60 ms (8°C over 100 ms). This finding was because the post-irradiation temperature difference between the epidermis and superficial dermis was reduced when the surface was cooled (Fig. 7). Such a result is in apparent disagreement with previous experimental data, which indicated that for cooled tissue, the surface temperature increased dramatically during the laser pulse (τ_p = 0.45 ms), and returned to initial (baseline) temperature within milliseconds [6]. The discrepancy in results may be explained by recent studies in which it was demonstrated that for cooling durations of 50–100 ms, the duration of the cooling occurred was tens to hundreds of milliseconds longer than the spray duration [9,12] because of a residual cryogen/ice layer on the tissue surface. Numerical studies have simulated CSC pulses as being uniform in intensity over time, and stopped cooling at laser onset [15,17] or continued it unchanged during and after the laser pulse [11]. In the future, boundary conditions used to simulate CSC may need to be altered to account for residual cooling, which tapers off after the end of a cryogen spurt.

Several previous studies have incorporated radiometric surface temperature measurement during CSC. In one study, surface temperatures were shown to be reduced by 30–40°C for spurt durations between 5 and 80 ms [14]. A more recent investigation indicated a temperature reduction of 25–40°C for pulse durations of 20–100 ms [16]. Our model indicated post-irradiation surface temperature reductions of 24°C for D_{csc} = 20 ms

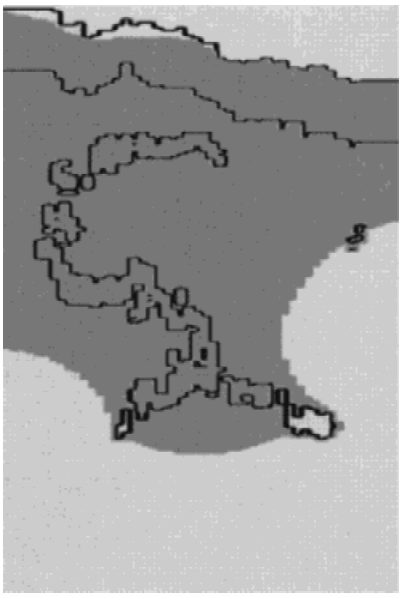

Fig. 9. Distribution of native (light gray) and coagulated (dark gray) tissue after the end of the relaxation phase for continuous cooling simulation.

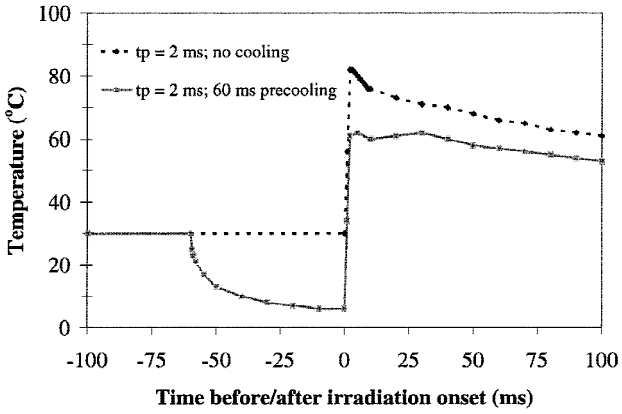

Fig. 10. Transient temperature distributions at the epidermal surface for τ_p = 2 ms with no cooling (dashed line); and τ_p = 2 ms with D_{csc} = 60 ms (gray solid line).

and 27°C for D_{csc} = 60 ms. The discrepancy between these data sets may be caused by variations in temperature and thickness of the ice/cryogen layer on the skin surface. However, radiometric data published recently by Torres et al. [12] indicated better agreement with our results — a surface temperature reduction of 28°C at the end of a 40 ms CSC spurt. In a recent in vivo study of CSC in hamster skin, temperature reductions of 5–10°C were recorded for a cooling pulse of 100 ms with a thermocouple located 625 μm below the tissue surface [33]. These results indicate a much deeper cooling effect than that seen in the present simulations, possibly due to significant anatomic and physiological differences between human and hamster skin or the finite thickness of the skin preparation.

Previous theoretical studies have predicted the temperature response versus skin depth in response to CSC. One study indicated that a 20-ms cooling pulse caused a decrease of 10°C at a depth of ~60 μm, whereas a 60 ms pulse resulted in a 10°C reduction to depths greater than 100 μm [16]. Another study indicated that post-irradiation temperatures might decrease by nearly 10°C down to a depth of 200 μm, for typical clinical laser parameters (τ_p = 0.5 ms, λ = 585 nm) and CSC durations of 80–100 ms [17]. Both of these studies are in reasonable agreement our results, although differences in laser parameters make accurate comparisons difficult.

Optimization of Treatment Parameters

Our simulations indicated that the threshold radiant exposure for epidermal injury at τ_p = 2 ms was approximately 6 J/cm^2. This rate is in reasonable agreement with the finding of a previous theoretical study that, in patients with type II skin (intermediate melanin content), no cooling was required for epidermal preservation for a radiant exposure (H_o) of 5 J/cm^2, whereas for higher radiant exposures, a longer spurt duration was required to avoid coagulation [17]. Within the limited parameter space investigated in the present study, the optimal pulse duration for this PWS was found to be 2 ms and the optimal CSC spurt duration was 60 ms. This combination of parameters should provide vascular and perivascular coagulation to a depth of approximately 300 μm, without epidermal coagulation. The authors are not aware of any previous study that has theoretically or experimentally evaluated PWS treatment by using this combination of laser and cooling parameters; however, laser pulse durations on the order of 2 ms have been identified as optimal for noncooled treatment in several previous studies [3,19,34–36].

Our results indicate that τ_p not only has a significant influence on vessel coagulation, but on the efficacy of CSC for epidermal sparing as well. To produce a specific maximum temperature in a small blood vessel (such as the 20- to 30-μm diameter vessels typical of the PWS used in this study), an increase in τ_p must typically be accompanied by an increase in radiant exposure. However, due to the air-tissue (adiabatic) boundary condition and low thermal conductivity in the epidermis, epidermal temperatures are approxi-

mately proportional to radiant exposure. The impact of CSC is reduced in the epidermis as laser pulse duration increases because the cooling effect becomes more distributed within the tissue (Figs. 6–8), causing a reduction in the extent of coagulation in deeper regions (Fig. 4c,f,i). Thus, safe CSC/laser treatments may be more difficult to achieve when pulse durations of 10 ms or greater are used. However, it must be noted that the apparent superiority of shorter laser pulse treatment may be reduced or eliminated when treatment involves irradiation of blood vessels with more typical PWS diameters of 50–120 μm.

Figure 8 also documents the results of a simulation involving continuous cooling (including 60 ms of pre-irradiation cooling), which was used to investigate a possible methodology for minimizing the excessive temperatures and coagulation seen for τ_p = 10 ms. Continuous cooling produced a skin surface temperature at least 55°C less than the other CSC cases at τ_p = 10 ms. However, by a depth of about 70 μm, the difference in temperature between D_{csc} = 60 ms and the continuous case was minimal (4°C). Thus, only part of the most superficial epidermal regions remained native. Although these results seem to indicate that continuous or postcooling would have little effect on tissue damage, it is worthwhile to consider that for longer pulse durations, larger tissue volumes reached temperatures at or exceeding the threshold for coagulation, which led to longer thermal relaxation times. As indicated by Figure 2, if the exposure duration increases, then the threshold temperature becomes reduced and coagulation may occur. Therefore, post-irradiation cooling may be most important for longer laser pulse durations.

The use of a maximum temperature end point (150°C) in this study was problematic in that it produced a 10-ms pulse duration case in which extensive coagulation was predicted. This outcome did not represent the best possible treatment result. This result is interesting because previous studies that have used threshold temperature-based end points have typically not presented information on collateral damage [3,28, 29]. In future studies, it may be more appropriate to consider coagulation of a specified percentage of vessel (or vessel wall) regions as the end point, based on the Arrhenius equation.

Our results indicate that to more accurately estimate the thermal mechanisms in the epidermis, it may be important to account for the variation in absorption across its layers. Because a significant portion of epidermal melanin is contained in deeper layers, which can be 50–100 μm deep and vary from patient to patient [3], it may be worthwhile to investigate a variety of epidermal morphologies. Computational investigation of several combinations of precooling and postcooling durations and delay periods may also be useful in identifying optimal treatment parameters for a specific PWS anatomy.

CONCLUSIONS

A 3-D optical-thermal numerical model has been implemented to study the effect of CSC on simulated laser treatment of PWS by using tissue morphology specified from a true PWS biopsy. Results were obtained for laser pulse durations of 0.5, 2, and 10 ms (λ = 585 nm) in conjunction with 20- and 60-ms-long CSC (precooling) spurts as well as noncooled irradiations. The use of continuous cooling during irradiation was also simulated.

The most important findings of this study include (1) The effect of CSC cooling was confined to the most superficial 100–200 μm, particularly for shorter laser pulses; (2) As the cryogen spurt duration was increased from 20 ms to 60 ms, the pre-irradiation temperature reduction at the dermoepidermal junction increased from 7°C to 12°C; (3) Superficial skin temperatures were significantly effected by the low thermal conductivity of the epidermis; (4) Of the treatment parameters investigated in this study, the optimal laser pulse length and CSC spurt duration (for this specific PWS morphology) were 2 ms and 60 ms, respectively; and, (5) CSC was most effective for epidermal temperature reduction during shorter laser pulses, but more necessary for longer laser pulse durations.

When planning CSC/laser treatment of PWS, tissue morphology and laser pulse duration should be taken into account. The results of this study indicate that our novel modeling technique has significant promise as a tool for improving understanding of laser-tissue interactions in highly nonhomogeneous tissue and optimizing laser and cooling parameters on an individual patient basis.

ACKNOWLEDGMENT

A.J. Welch is the Marion E. Forsman Professor of Electrical and Computer Engineering.

REFERENCES

1. Anderson RR, Parrish JA. Selective photothermolysis: precise microsurgery by selective absorption of pulsed radiation. Science 1983;220:524–527.
2. Anderson RR. Laser-tissue interactions. In: Goldman MP, Fitzpatrick RE, editors. Cutaneous laser surgery: the art and science of selective photothermolysis. St. Louis: Magby; 1994.
3. van Gemert MJC, Welch AJ, Pickering JW, Tan OT. Laser treatment of port wine stains. In: Welch AJ, van Gemert MJC, editors. Optical-thermal response of laser-irradiated tissue. New York: Plenum Press; 1995.
4. Gilchrest BA, Rosen S, Noel JM. Chilling port wine stains improves the response to argon laser therapy. Plast Reconstr Surg 1982;69:278–283.
5. Welch AJ, Motamedi M, Gonzalez A. Evaluation of cooling techniques for the protection of the epidermis during Nd-YAG laser irradiation of the skin. In: Joffe SN, editor. Neodymium-YAG laser in medicine and surgery. New York: Elsevier; 1983.
6. Nelson JS, Milner TE, Anvari B, Tanenbaum BS, Kimel S, Svaasand LO, Jacques SL. Dynamic epidermal cooling during pulsed laser treatment of port-wine stain. Arch Dermatol 1995;131:695–700.
7. Hohenleutner U, Walther T, Wenig M, Baumler W, Landthaler M. Leg telangiectasia treatment with a 1.5 ms pulsed dye laser, ice cube cooling of the skin and 595 vs 600 nm: preliminary results. Lasers Surg Med 1998;23: 72–78.
8. Chess C, Chess Q. Cool laser optics treatment of large telangiectasia of the lower extremities. J Dermatol Surg Oncol 1993;19:74–80.
9. Exley J, Dickinson M, King T, Charlton A, Falder S, Kenealy J. Comparison of cooling criteria with a cryogen spray and water/air spray. Proc SPIE 1999;3601:130–140.
10. Strauss JS, Kligman AM. Observations on dermabrasion and the anatomy of the acne pit. Arch Dermatol 1956;74: 397–404.
11. Nelson JS, Milner TE, Anvari B, Tanenbaum BS, Svaasand LO, Kimel S. Dynamic epidermal cooling in conjunction with laser-induced photothermolysis of port wine stain blood vessels. Lasers Surg Med 1996;19:224–229.
12. Torres JH, Anvari B, Tanenbaum BS, Milner TE, Yu JC, Nelson JS. Internal temperature measurements in response to cryogen spray cooling of a skin phantom. Proc SPIE 1999;3590:11–19.
13. Incropera FP, DeWitt DP. Fundamentals of heat and mass transfer. 4th ed. New York: John Wiley & Sons; 1996.
14. Anvari B, Milner TE, Tanenbaum BS, Kimel S, Svaasand LO, Nelson JS. Selective cooling of biological tissues: application for thermally mediated therapeutic procedures. Phys Med Biol 1995;40:241–252.
15. Anvari B, Milner TE, Tanenbaum BS, Kimel S, Svaasand LO, Nelson JS. Dynamic epidermal cooling in conjunction with laser treatment of port-wine stains: theoretical and preliminary clinical evaluations. Lasers Med Sci 1995;10: 105–112.
16. Anvari B, Milner TE, Tanenbaum BS, Nelson JS. A comparative study of human skin thermal response to sapphire contact and cryogen spray cooling. IEEE Trans Biomed Eng 1998;45:934–941.
17. Anvari B, Milner TE, Tanenbaum BS, Kimel S, Svaasand LO, Nelson JS. A theoretical study of the thermal response of skin to cryogen spray cooling and pulsed laser irradiation: implications for treatment of port wine stain birthmarks. Phys Med Biol 1995;40:1451–1465.
18. Sturesson C, Andersson-Engels S. Mathematical modelling of dynamic cooling and pre-heating used to increase the depth of selective damage to blood vessels in laser treatment of port wine stains. Phys Med Biol 1996;41: 413–428.
19. Pfefer TJ, Barton JK, Smithies DJ, Milner TE, Nelson JS, van Gemert MJC, Welch AJ. Modeling laser treatment of port wine stains with a computer-reconstructed biopsy. Lasers Surg Med 1999;24:151–166.
20. Smithies DJ, van Gemert MJC, Hansen MK, Milner TE, Nelson JS. Three-dimensional reconstruction of port wine stain vascular anatomy from serial histological sections. Phys Med Biol 1997;42:1843–1847.
21. Pfefer TJ, Barton JK, Chan EK, Ducros MG, Sorg BS, Milner TE, Nelson JS, Welch AJ. A three dimensional modular adaptable grid numerical model for light propagation during laser irradiation of skin tissue. IEEE J Sel Top Quantum Electron 1996;2:934–942.
22. Barton JK, Pfefer TJ, Welch AJ, Smithies DJ, Nelson JS, van Gemert MJC. Optical Monte Carlo modeling of a true port wine stain anatomy. Optics Express 1998; 2:391–396.
23. Duck FA. Thermal properties of tissue. In: Physical properties of tissue. London: Academic Press; 1990.
24. Moritz AR, Henriques FC Jr. Studies in thermal injury II. The relative importance of time and surface temperature in the causation of cutaneous burns. Am J Pathol 1947; 23:695–720.
25. Pearce J, Thomsen S. Rate process analysis of thermal damage. In: Welch AJ, van Gemert MJC, editors. Optical-thermal response of laser-irradiated tissue. New York: Plenum Press; 1995.
26. Lepock JR, Frey HE, Bayne H, Markus J. Relationship of hyperthermia-induced hemolysis of human erythrocytes to the thermal denaturation of membrane proteins. Biochim Biophys Acta 1989;980:191–201.
27. Weaver JA, Stoll AM. Mathematical model of skin exposed to thermal radiation. Aerosp Med 1969; 40:24.
28. de Boer JF, Lucassen GW, Verkruysse W, van Gemert MJC. Thermolysis of port-wine-stain blood vessels: diameter of a damaged blood vessel depends on the laser pulse length. Lasers Med Sci 1996;11:177–180.
29. Kimel S, Svaasand LO, Hammer-Wilson M, Schnell MJ, Milner TE, Nelson JS, Berns MW. Differential vascular response to laser photothermolysis. J Invest Dermatol 1994;103:693–700.
30. LeCarpentier G, Motamedi M, McMath L, Rastegar S, Welch A. Continuous wave laser ablation of tissue: analysis of thermal and mechanical events. IEEE Trans Biomed Eng 1993;40(2):188–199.
31. Pfefer TJ, Choi B, Vargas G, McNally KM, Welch AJ. Mechanisms of pulsed laser-induced thermal coagulation of whole blood in vitro. Proc SPIE 1999; 3590:20–31.
32. Miller ID, Veitch AR. Optical modelling of light distribu-

tions in skin tissue following laser irradiation. Lasers Surg Med 1993;13:565–571.
33. Vargas G, Barton JK, Choi B, Izatt JA, Welch AJ. Assessing vessel damage with color Doppler optical coherence tomography. Proc SPIE 1999;3598:185–194.
34. Anderson RR, Parrish JA. Microvasculature can be selectively damaged using dye lasers: a basic theory and experimental evidence in human skin. Lasers Surg Med 1981;1:263–276.
35. Smithies DJ, Butler PH. Modelling the distribution of laser light in port-wine stains with the Monte Carlo method. Phys Med Biol 1995;40:701–731.
36. Pickering JW, Butler PH, Ring BJ, Walker EP. Computed temperature distributions around ectatic capillaries exposed to yellow (578 nm) laser light. Phys Med Biol 1989;34:1247–1258.
37. McNally KM, Optical and thermal studies of laser solder tissue repair in vitro. Ph.D. Thesis, School of Mathematics, Physics, Computing and Electronics. 1998, Macquarie University: Sydney, Australia.
38. Agah R, Pearce JA, Welch AJ, Motamedi M. Rate process model for arterial tissue thermal damage: implications on vessel photocoagulation. Lasers Surg Med 1994;15: 176–184.
39. Henriques FC, Jr. Studies in thermal injury V. The predictability and significance of thermally induced rate processes leading to irreversible epidermal injury. Arch Pathol 1947;43:489–502.